

# ELECTROCHEMICAL PROPERTIES ENHANCEMENT OF SPINEL LITHIUM NICKEL MANGANESE OXIDE BY SECONDARY HEAT TREATMENT AND ASSISTANT PHASE FORMATION

Mai Thanh Tung, Do Xuan Giang\*

<sup>1</sup>Department of Electrochemistry and Corrosion Protection, School of Chemical Engineering,  
Hanoi University of Science and Technology

Received 5 March 2015; Accepted for Publication 20 April 2015

## Abstract

LiNi<sub>x</sub>Mn<sub>2-x</sub>O<sub>y</sub> as cathode materials discharge at 4.7 V versus Li<sup>+</sup>/Li potential produced high stability of structures during lithium insertion/extraction. The supplement of Ni amount of  $x > 0.5$  appeared the secondary cubic phase of hexa-nickel Manganese Oxide which assisted the material increase the electrochemical performance. The additional heat treatment at 700 °C for 36 hours of two phases LiNi<sub>0.5</sub>Mn<sub>1.5</sub>O<sub>4</sub> and Ni<sub>6</sub>MnO<sub>8</sub> enhances cycle ability of entire materials.

**Keywords.** Lithium-ion batteries, Spinel, Cathode materials, Energy, XRD analysis.

## 1. INTRODUCTION

The lithium manganese-nickel oxide spinel as a high voltage cathode material for Li-ion rechargeable battery has received a lot of attention due to their high energy storage as well as their thermodynamic stability during charge-discharge processes. The main electrode reaction is occurred by the variation of the nickel oxidation state from Ni(II) to Ni(IV), along with the de-intercalation of Li-ion out of the spinel structure and vice versa. This process happens at voltage range  $\approx 4.7V$  vs. Li [1-3].

The effect of Mn:Ni proportion in compound with Ni < 0.5 was also investigated and then created the series of spinel composites which had the electrochemical behaviors like LiMn<sub>2</sub>O<sub>4</sub> with Ni < 0.25 and/or intermediary between LiMn<sub>2</sub>O<sub>4</sub> and LiMn<sub>1.5</sub>Ni<sub>0.5</sub>O<sub>4</sub> with  $0.25 < Ni < 0.5$  [5]. There has been no study with the contribution of higher than 0.5 of nickel, and otherwise, to pursue the target of enhanced the power performance but to be undamaged to the cycle ability, the series of samples with more than 0.5 supplement of Ni amount were investigated. The results of the formation of new metal oxide phase of nickel which affect to the entire cathode materials were reported.

## 2. EXPERIMENTAL

In this work, the LiMn<sub>2-x</sub>Ni<sub>x</sub>O<sub>y</sub> materials were

synthesized by solid state reactions. The stoichiometric amounts of Mn<sub>2</sub>O<sub>3</sub> (99 % Aldrich), Ni(CH<sub>3</sub>COO)<sub>2</sub>·4H<sub>2</sub>O (98 % Aldrich) and LiOH (98 % Aldrich) with  $x = 0.5; 0.75$  and  $1.0$  were first mixed by ball-milling method for 12h before being calcined at 1000 °C for 24 h in air. The resulting products then ground and collected for other experiments. A part of them were given into the furnace for the secondary heat treatment at 700 °C for 36 h in air.

Powder X-ray diffraction (XRD) pattern were step-scan-recorded on a X'Pert PRO Multi Purpose X-Ray Diffractometer equipped with CuK<sub>α</sub> radiation ( $\lambda = 1.5406 \text{ \AA}$ ) in step of 0.02° with 1°/min over the range  $10^\circ < 2\theta < 80^\circ$  for each samples. The particles morphology and manganese/nickel distribution were studied using field-emission scanning electron microscope (FE-SEM) and Energy Dispersive X-ray (EDX) mapping (S-4700/EX-200 Hitachi).

The electrochemistry of those samples was investigated in the standard CR2032 coin cells with LiPF<sub>6</sub> in ethylene carbonate (EC)/dimethyl carbonate (DMC) 1:1 as electrolyte. The anode was lithium foil and cathode was prepared by mixing 70 wt% of active material, 20 wt% of carbon black, and 10 wt% of teflonized acetylene black binder. The cells were assembled in the Ar-filled glove box and tested at room temperature using a BTS 2004H (Nagano, Japan).

## 3. RESULTS AND DISCUSSION

XRD patterns of these samples with and without the secondary heat treatment were shown respectively in Fig. 1a and Fig. 1b, and revealed the main phase was Spinel structure of  $\text{LiMn}_{1.5}\text{Ni}_{0.5}\text{O}_4$  compound. The previous reports suggested that its crystal structure belongs to the space group Fd-3m or P4<sub>3</sub>32 for disorder or order type [4, 5]. The new raising peaks when the nickel ratio increasing

indicated more probably the structure of cubic  $\text{Ni}_6\text{MnO}_8$ , with the specific peaks at 18.6°, 21.5° and 30.6° than the rock-salt  $\text{Li}_x\text{Ni}_{1-x}\text{O}$  compounds, which are without those peaks in their XDR profiles. There was not much the change of XRD data after heat treatment except the disappearance of the peak at 44.2°, may be related to  $\text{Li}_x\text{Ni}_{1-x}\text{O}$  phase transformation in the Mn:Ni 1:1 sample. The concentration of  $\text{Ni}_6\text{MnO}_8$  increased when rising ratio of nickel in powders.

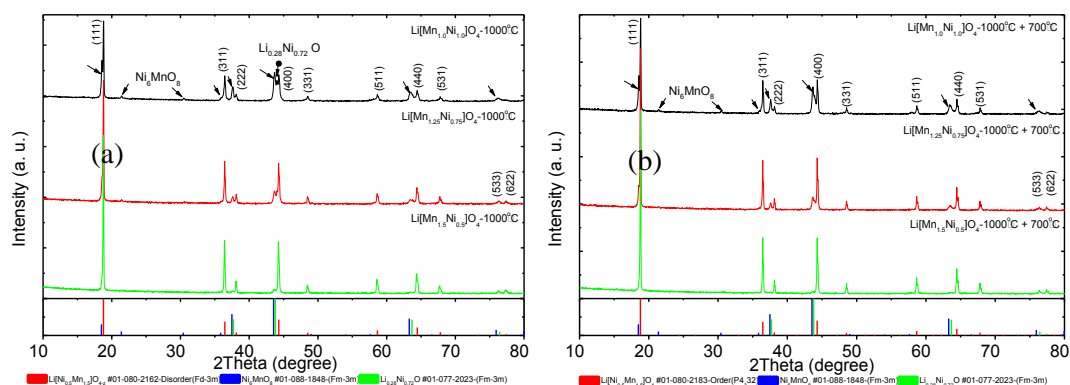


Figure 1: The X-ray diffraction patterns of the pre- and post-secondary heat treatment (a), (b), and these analysis (c), (d), respectively. The bottom column charts (a, b) show the peaks copyright from JCPDS, ICDD database

The FE-SEM and EDX mapping in Fig. 2(a-f) shows that the samples consist of polygonal particles and are characterized by high crystallinity material and synthesized by solid state reaction. The particles sizes of all three samples before and after secondary heat treatment are between 4-10  $\mu\text{m}$ . The EDX mapping provides more detail compositions of each primary particle which is not present as a separate compound. Each particle exhibits regions with the different elemental distributions. The region with more red dots (nickel rich) may be  $\text{Ni}_6\text{MnO}_8$  secondary particle and the more green dots region (manganese rich) may suggest the existence of  $\text{LiMn}_{1.5}\text{Ni}_{0.5}\text{O}_4$  secondary particle. Since the unit cell parameters of the two compounds are pretty similar as well as the same cubic type, it is inferred that they can easily share the grain boundary without problems, and  $\text{Ni}_6\text{MnO}_8$  in the compound should assist the stability of whole structure during  $\text{LiMn}_{1.5}\text{Ni}_{0.5}\text{O}_4$  perform in charge/discharge work. It seems happening the re-arrangement the order of phases whereby the compound which has manganese-rich floats onto the near surface of the particles and the nickel-rich compound may be settled down into the deeper layers, after heat treatment at 700 °C in 36 hours, with the 0.75 Ni

sample. For other samples, there was nothing happened during secondary heat.

The electrochemical reversible insertion/extraction of Li ion on the present materials utilization as the cathode within the voltage 3.5-5.0 V under the current density of 0.025  $\text{mA}/\text{cm}^2$  in 2032 type test cells were shown in the Fig. 3(a-f). Overall, the first charged voltage curve of all samples indicates the double times of capacity higher than the next curves in order to reach 5 V vs. Li. This phenomenon can be explained by the activation of the conducting agents and the SEI formation at the cathode side in the high voltage condition [2, 5] and happens only to the first charged and do not affect obviously to the next charge/discharge processes. Before heating at 700 °C for 36 hours, the voltage profiles of three samples reveal the similar trends with three plateaus. The first and second plateaus occur on very narrow voltage range between 4.75-4.55 V during discharging due to the reductions of  $\text{Ni}^{4+}$  to  $\text{Ni}^{3+}$  and  $\text{Ni}^{3+}$  to  $\text{Ni}^{2+}$ , respectively, enclose with the lithium intercalation in the disorder spinel structure (Fd-3m space group) of  $\text{LiMn}_{1.5}\text{Ni}_{0.5}\text{O}_{4-\delta}$ . The third plateau is a token at 4.0 V represents for  $\text{Mn}^{4+}$  to  $\text{Mn}^{3+}$  reduction and also demonstrates the presence of  $\text{Mn}^{3+}$  in spinel structure. The first cycle capacity

decreases of 148, 110 and 80 mAh/g following by the rise of nickel contents of 0.5, 0.75 and 1.0 in molar ratio. After 100 cycles, the material with 0.5

Ni reaches 92 % of capacity retention, comparing with 96 % for 0.75 Ni and 73 % for 1.00 Ni materials.

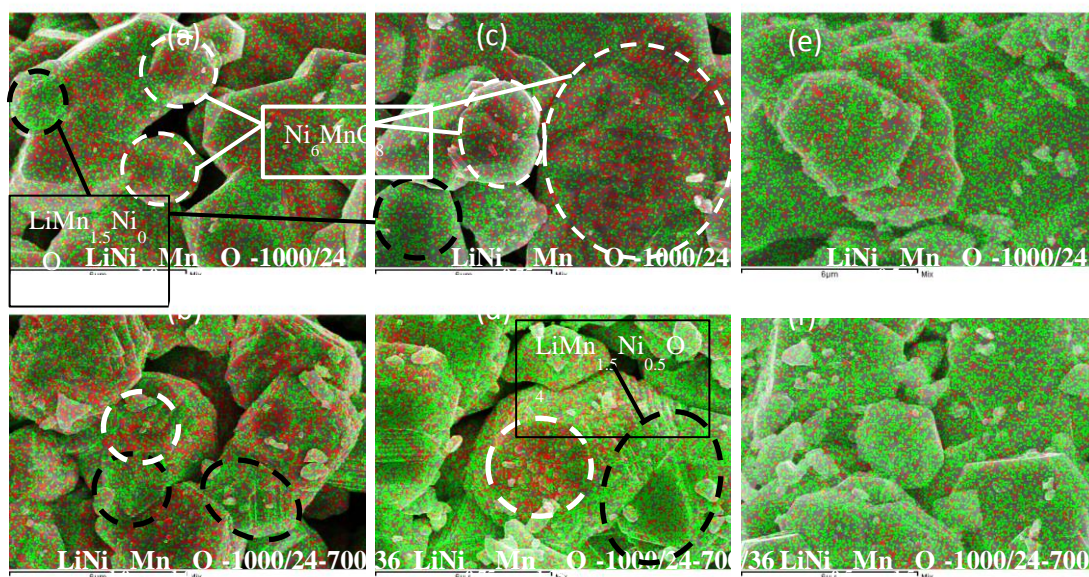


Figure 2: The FE-SEM and EDX mapping of before and after heating at 700 °C for 36 hours in air  $\text{LiMn}_{2-x}\text{Ni}_x\text{O}_y$  samples as  $x = 1.00$  (a, b); 0.75 (c, d) and 0.5 (e, f)

The electrochemical reversible insertion/extraction of Li ion on the present materials utilization as the cathode within the voltage 3.5-5.0 V under the current density of 0.025 mA/cm<sup>2</sup> in 2032 type test cells were shown in the Fig. 3(a-f). Overall, the first charged voltage curve of all samples indicates the double times of capacity higher than the next curves in order to reach 5V vs. Li. This phenomenon can be explained by the activation of the conducting agents and the SEI formation at the cathode side in the high voltage condition [2, 5] and happens only to the first charged and does not affect obviously the next charge/discharge processes. Before heating at 700 °C for 36 hours, the voltage profiles of three samples reveal the similar trends with three plateaus. The first and second plateaus occur on very narrow voltage range between 4.75-4.55 V during discharging due to the reductions of Ni<sup>4+</sup> to Ni<sup>3+</sup> and Ni<sup>3+</sup> to Ni<sup>2+</sup>, respectively, enclose with the lithium intercalation in the disorder spinel structure (Fd-3m space group) of  $\text{LiMn}_{1.5}\text{Ni}_{0.5}\text{O}_{4-\delta}$ . The third plateau is a token at 4.0 V represents for Mn<sup>4+</sup> to Mn<sup>3+</sup> reduction and also demonstrates the presence of Mn<sup>3+</sup> in spinel structure. The first cycle capacity decreases of 148, 110 and 80 mAh/g following by the rise of nickel contents of 0.5, 0.75 and 1.0 in molar ratio. After 100 cycles, the material with 0.5 Ni reaches 92 % of capacity retention, comparing

with 96 % for 0.75 Ni and 73 % for 1.00 Ni materials.

In contrast, the samples with secondary heat treatment at 700 °C for 36 hours index only one plateau at 4.7V range characterized by Ni<sup>4+</sup>/Ni<sup>2+</sup> redox couple in the order type spinel structure (P4<sub>3</sub>32 space group) of  $\text{LiMn}_{1.5}\text{Ni}_{0.5}\text{O}_4$ . Based on the plot of stoichiometric material with the Ni ratio at 0.5, it still remains the small quantity of Mn<sup>3+</sup>. On the other hand, the presence of Ni<sub>6</sub>MnO<sub>8</sub> phase which had a fixed of oxidative states of manganese at +4 and nickel at +2 during the heat variation may assist the enhancement of structure stability for the materials, by the compensation of the oxygen deficient part. The mechanism of the assistance has not been studied, but the figures 3e, f indicated the evidences that most of manganese (III) cations were eliminated from the structures, and since the rearrangement of crystal order where the spinel  $\text{LiMn}_{1.5}\text{Ni}_{0.5}\text{O}_4$  phase float onto the particles' surface has been occurred, the first delivered capacity of the 0.75 Ni sample reached the significant improvement of approx. 10 mAh/g higher than the sample without heat treatment. In the opposite way, the sample with 0.5 Ni exhibited more rapid fading of capacity comparing to the pre-heating sample. The capacity retention is only 90 % after 100 cycles.

The various current rates were applied and the results showed in the Fig. 3h. For the sample with

0.5 Ni, the electrochemical performances come similarly the earlier reports which explained that due to the lack of  $Mn^{3+}$  after annealing at 700 °C, the acceleration of Li cations insertion was limited [4]. Up to 1.6 mA/cm<sup>2</sup> (approximately 6C for the ideal spinel  $LiMn_{1.5}Ni_{0.5}O_4$  material), the capacities were remaining 50 and 44 mAh/g before and after powders heating at 700 °C, respectively. In contrast, the materials contained secondary phase of  $Ni_6MnO_8$  showed the different trend. After heating, the capacities retention versus the increasing variation of currents is considerably better than that of before

heating. At the current density of 1.6mA/cm<sup>2</sup> the delivered capacities of the samples before and after secondary heat treatment are 35 and 62 mAh/g for 0.75 Ni materials and/or 10 and 23 mAh/g for 1.00 Ni materials. At the higher current density, it seems to reach critically discharging of the materials; hence, capacities left down very fast and mostly undelivered at 10 mA/cm<sup>2</sup>. All the examined cathode materials showed robustly the rehabilitation of energy while the applied current density restored to 0.05 mA/cm<sup>2</sup>.

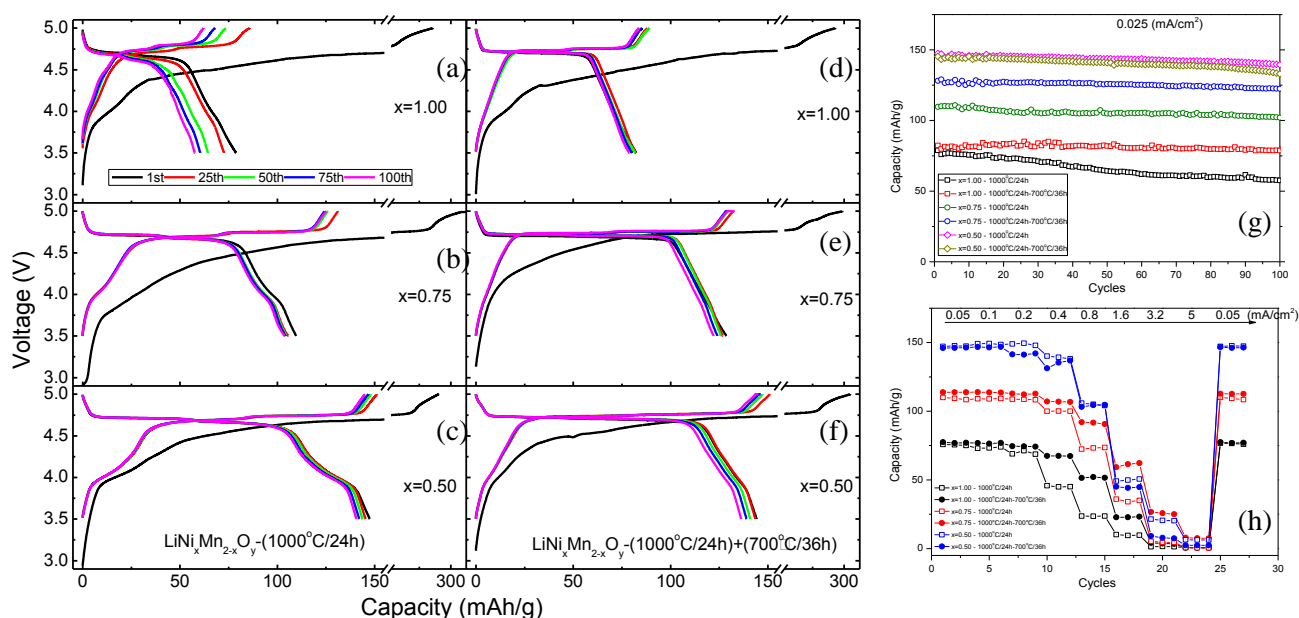


Figure 3: Galvanostatic charge/discharge curves of  $LiMn_{2-x}Ni_xO_y$  at 25 °C and 0.025 mA/cm<sup>2</sup>(a-f). Cycleability (g) up to 100 cycles and C-rate performance (h)

#### 4. CONCLUSION

The high nickel quantity of Lithium Nickel Manganese Oxides composites at different heating processes were synthesized and comparatively studied. By additional heating at 700 °C for 36 hours and the appropriately increasing variation of Ni amount to form the assistant phase of  $Ni_6MnO_8$ , beside the active spinel  $LiMn_{1.5}Ni_{0.5}O_4$  being evidenced by XRD and EDX mapping, the composites indicated the decrease of first delivered capacities whereas improved the cycle abilities and enhanced the current performances. After secondary heat treatment, there was the structural transformation of active spinel phase from the disorder type (Fd-3m)  $LiMn_{1.5}Ni_{0.5}O_{4-\delta}$  to order type (P4<sub>3</sub>2)  $LiMn_{1.5}Ni_{0.5}O_4$  and the presence of assistant phase helped this process occurring more completely, by the disappearance of  $Mn^{4+}/Mn^{3+}$  reduction to the voltage profiles. The SEM and EDX

mapping showed evidence of the phases' rearrangement happening in  $LiMn_{1.25}Ni_{0.75}O_y$  composite where the  $LiMn_{1.5}Ni_{0.5}O_4$  floated over the particles' surface while the assistant  $Ni_6MnO_8$  phase deepened into their centre during heat treatment. The stability of the assistant phase under high voltage was demonstrated by ability to enduringly deliver up to 100 cycles of these materials.

#### REFERENCES

1. K. Amine, H. Tukamoto, H. Yasuda, Y. Fujita. J. Electrochem. Soc., **143**, 1607 (1996).
2. T. Ohzuku, S. Takeda, M. Iwanaga. J. Power Sources **81-82**, 90 (1999).
3. M. Kunduraci, G. G. Amatucci. J. Power Sources, **165**, 359 (2007).
4. Y. Idemoto, H. Narai, N. Koura. J. Power Sources, **119-121**, 125 (2003).
5. H. M. Wu, J. P. Tu, X. T. Chen, D. Q. Shi, X. B. Zhao, G. S. Cao. Electrochim. Acta, **51**, 4148 (2006).

